The Intraflavin Hydrogen Bond in Human Electron Transfer Flavoprotein Modulates Redox Potentials and May Participate in Electron Transfer†

Timothy M. Dwyer,‡ Simone Mortl,§ Kristina Kemter,§ Adelbert Bacher,§ Abdul Fauq,|| and Frank E. Frerman*,‡

Department of Pediatrics and the Cell and Developmental Biology Program, University of Colorado School of Medicine, Denver, Colorado 80262, Lehrstuhl fur Organische Chemie und Biochemie, Technische Universitat, Munchen, Germany, and the Mayo Clinic, Jacksonville, Florida 32224

Received February 18, 1999; Revised Manuscript Received May 17, 1999

ABSTRACT: Electron-transfer flavoprotein (ETF) serves as an intermediate electron carrier between primary flavoprotein dehydrogenases and terminal respiratory chains in mitochondria and prokaryotic cells. The three-dimensional structures of human and *Paracoccus denitrificans* ETFs determined by X-ray crystallography indicate that the 4′-hydroxyl of the ribityl side chain of FAD is hydrogen bonded to N(1) of the flavin ring. We have substituted 4′-deoxy-FAD for the native FAD and investigated the analog-containing ETF to determine the role of this rare intra-cofactor hydrogen bond. The binding constants for 4′-deoxy-FAD and FAD with the apoprotein are very similar, and the energy of binding differs by only 2 kJ/mol. The overall two-electron oxidation−reduction potential of 4′-deoxy-FAD in solution is identical to that of FAD. However, the potential of the oxidized/semiquinone couple of the ETF containing 4′-deoxy-FAD is 0.116 V less than the oxidized/semiquinone couple of the native protein. These data suggest that the 4′-hydoxyl-N(1) hydrogen bond stabilizes the anionic semiquinone in which negative charge is delocalized over the N(1)−C(2)O region. Transfer of the second electron to 4′-deoxy-FAD reconstituted ETF is extremely slow, and it was very difficult to achieve complete reduction of the flavin semiquinone to the hydroquinone. The turnover of medium chain acyl-CoA dehydrogenase with native ETF and ETF containing the 4′-deoxy analogue was essentially identical when the reduced ETF was recycled by reduction of 2,6-dichlorophenolindophenol. However, the steady-state turnover of the dehydrogenase with 4′-deoxy-FAD was only 23% of the turnover with native ETF when ETF semiquinone formation was assayed directly under anaerobic conditions. This is consistent with the decreased potential of the oxidized semiquinone couple of the analog-containing ETF. ETF containing 4′-deoxy-FAD neither donates to nor accepts electrons from electron-transfer flavoprotein ubiquinone oxidoreductase (ETF-QO) at significant rates (≤0.5% the wild-type rates). These results indicate that the 4′-hydroxyl-N(1) hydrogen bond plays a major role in the stabilization of the anionic semiquinone and anionic hydroquinone oxidation states of ETF and that this hydrogen bond may provide a pathway for electron transfer between the ETF flavin and the flavin of ETF-QO.

Electron-transfer flavoprotein (ETF)[1] functions as the site for input of electrons from nine flavoprotein dehydrogenases into the mammalian respiratory chain via electron-transfer flavoprotein ubiquinone oxidoreductase (ETF-QO) and ubiquinone. The primary flavoprotein dehydrogenases include four chain-length specific acyl-CoA dehydrogenases in fatty acid β-oxidation (*1*, *2*) and the related acyl-CoA dehydrogenases that function in the mitochondrial oxidation of leucine, valine, isoleucine, and lysine (*3*, *4*). Two *N*-methyl flavoprotein dehydrogenases, dimethylglycine dehydrogenase and sarcosine dehydrogenase, are also oxidized by ETF (*5*). The ETF flavin is reduced to the anionic semiquinone by all of the two-electron-reduced primary dehydrogenases in one-electron transfer steps (*6*). Transfer of a second electron to ETF semiquinone by the primary dehydrogenases is not kinetically significant (*6*, *7*).

Human ETF, like all members of the ETF superfamily (*8*, *9*, and references therein), is a heterodimeric, FAD-containing protein that also contains 1 equiv of noncovalently bound 5′-AMP in the β subunit. The mononucleotide apparently plays a role in the folding and dimerization of the human protein and related bacterial proteins (*10*−*13*). The X-ray crystal structures of human and *Paracoccus denitrificans* ETFs have recently been solved, and the three-dimensional structures are virtually identical (*9*, *14*). FAD is bound primarily in the αII domain of the larger (α) subunit, although the C7 and C8 methyl groups of the flavin xylene ring make van der Waals contact with Tyr16 and Phe41-(human numbering) in the β subunit. The primary sequence of the αII domain and the amino acids whose side chains contact the flavin are highly conserved throughout the ETF superfamily (*9* and references therein). Further, the crystal

† This work was supported by NIH Grants DK49726 (FEF) and a Mental Retardation Research Center Grant, HD04024, to Stephen I. Goodman.

* To whom correspondence should be addressed. Email: frerman_f@defiance.uchsc.edu. Fax: 303-315-8080. Telephone: 303-315-7269.

‡ University of Colorado School of Medicine.

§ Technische Universitat.

|| The Mayo Clinic.

[1] Abbreviations: ETFs, electron-transfer flavoproteins; ETF-QO, electron-transfer flavoprotein ubiquinone oxidoreductase.

10.1021/bi9903906 CCC: $18.00
Published on Web 07/02/1999

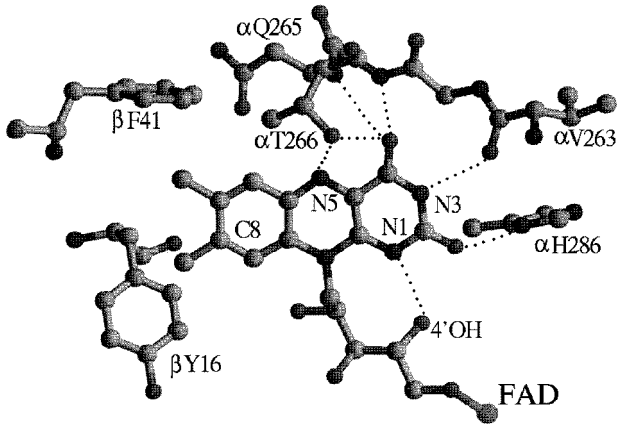

FIGURE 1: The interaction between FAD and the polypeptide in human ETF and the intraflavin hydrogen bond between the 4′-ribityl-hydroxyl and N(1) of the isoalloxazine ring. In the α subunit, the hydroxyl of T266, the imidazole N(1) of H286, the main chain amide nitrogens of T266 and R249 (not shown) are within hydrogen bonding distance of N(5) and the carbonyl oxygens at C(2) and C(4). The main chain carbonyl of V263 is within hydrogen bonding distance (2.8 Å) of N(3). The guanidinium group of R249 makes van der Waals contact with the xylene ring of the flavin. Y16 and F41 in the β subunit make van der Waals contact with the C(8) and C(7) methyl groups, respectively. The 4′-hydroxyl of the ribityl side chain is within hydrogen bonding distance (3.0 Å) of N(1) in the isoalloxazine ring.

structures suggested the presence of a rare type of intraflavin hydrogen bond between the 4′-ribityl hydroxyl and the flavin N(1) in the oxidized proteins. NMR spectroscopy of human ETF reconstituted with ^{13}C- and ^{15}N-enriched FAD shows that the oxidized and two-electron-reduced ETF flavin are strongly hydrogen bonded at N(1), N(5), and the carbonyl oxygens at C(2) and C(4) (*15*). These studies also showed that N(1) of the flavin is ionized in the two-electron-reduced state. The electron density of the anionic semiquinone and hydroquinones stabilized by human and *P. denitrificans* ETFs is delocalized over the N(1)-C(2)O region of the flavin, making hydrogen bonding in the region of N(1) and C(2)O important factors in the redox behavior of these ETFs.

Consistent with crystallographic studies (*9*, *14*), determinations of the NMR spectra of human ETF enriched with ^{13}C- and ^{15}N-FAD (*15*) indicated the presence of a rare hydrogen bond that may play a role in stabilizing the anionic semiquinone and hydroquinone of ETF flavin. The 4′-hydroxyl group of the ribityl side chain is within hydrogen bonding distance (3.0 Å) of N(1) of the flavin ring in both proteins (*9*, *14*). This hydrogen bond, and likely hydrogen bonds between the imidazole side chain of αH286, and the amide hydrogen of αR249 with the oxygen of the C(2) carbonyl of the flavin (Figure 1) may also contribute to the stabilization of the anionic semiquinone and anionic hydroquinone oxidation states.

The aims of this investigation were to obtain direct evidence for the intra-cofactor hydrogen bond and determine the function of the 4′-ribityl-hydroxyl-N(1) hydrogen bond on the stabilization of reduced forms of human ETF. 4′-Deoxy-FAD was synthesized, and human ETF was reconstituted with the FAD analogue. Loss of the hydrogen bond decreases the potentials of the ETF flavin redox couples as predicted by model studies (*16*, *17*) and experiments with a naturally occurring mutant human ETF lacking the αT266-flavin N(5) hydrogen bond (*18*). The analog-containing ETF serves as an electron acceptor for medium-chain acyl-CoA dehydrogenase; however, the ETF containing 4′-deoxy-FAD can neither donate electrons to nor accept electrons from ETF-QO at any significant rate, suggesting that this hydrogen bond may participate in an electron tunneling pathway between the two redox proteins. Considering the sequence identity of the FAD-containing domain throughout the ETF superfamily, the conservation of the three-dimensional structure between at least two members of this superfamily, and the conservation of amino acids in this domain that contact the flavin ring (*9*), the intraflavin hydrogen bond may also be conserved throughout the superfamily, and contribute to the redox behavior of the proteins.

EXPERIMENTAL PROCEDURES

Enzymes. Human ETF was expressed and purified as described by Griffin et al. (*15*), and the concentration was determined using $\epsilon_{436\ nm}$= 13 300 M $^{-1}$ cm^{-1} (*19*). Porcine medium-chain acyl-CoA dehydrogenase and porcine ETF-QO were purified as described (*20*, *21*), and protein concentrations were determined spectrophotometrically using $\epsilon_{448\ nm}$ = 15 400 M^{-1} cm^{-1} (*6*) and $\epsilon_{430\ nm}$ = 24 000 M $^{-1}$ (*21*), respectively. Pig heart submitochondrial particles were prepared as previously described by Frerman (*22*).

Synthesis of 4′-Deoxyriboflavin—General Methods. Nuclear magnetic spectra (^{1}H) were measured with a Bruker Wh-300 instrument (^{1}H frequency of 300 MHz) in the solvents noted. ^{1}H chemical shifts are expressed in parts per million downfield from Me_4Si, which was used as an internal standard. Column chromatography of intermediates was performed with silica gel (J. T. Baker, 40 μ). Anhydrous dimethyl formamide was obtained from Aldrich Chemicals. Tetrahydrofuran and diethyl ether were distilled over sodium benzophenone ketyl before use. Methylene chloride was distilled over calcium hydride or P_2O_5. All other chemicals were reagent grade and used without further treatment. The purity of all synthetic compounds is greater than 95% as judged by thin-layer chromatography and high-field ^{1}H NMR. Mass spectral analyses were performed at the Mayo Clinic Mass Spectroscopy Facility, Rochester, MN, and the Central Analytical Laboratory, University of Colorado, Boulder, CO.

*Step 1. Synthesis of (3aR,7S,7aR)-4-Methoxy-2,2-dimethylperhydro[1,3]dioxolo[4,5-c]pyran-7-ol (**3**) from* L-*Lyxose*. L-Lyxose (Aldrich) was dissolved in 300 mL of anhydrous methanol containing 0.5% anhydrous HCl and heated at 60 °C for 6 h. After the solution was cooled and neutralized with aqueous $NaHCO_3$, methanol was removed by rotary evaporation, and the product was extracted three times with diethyl ether. The combined ether layers were washed sequentially with water, brine, and anhydrous $MgSO_4$. The crude material was concentrated, dried over P_2O_5, and mixed with 250 mL of 2,2-dimethoxypropane and 4 mL of 4.5 M HCl in dioxane. After the solution was stirred for 3.5 h at room temperature, the reaction was quenched with 5 mL of trimethylamine, the solution was filtered, and the volatiles were removed under reduced pressure to give an oil. The oil was purified by flash chromatography (elution with 40−60% ethyl acetate/hexane) to furnish the hydroxyacetonide **3** (Scheme 1) as a thick oil (yield equaled 14.55 g, 78% in two steps). ^{1}H NMR ($CDCl_3$) 4.65 (1H, J = 2.7 Hz), 4.24

Scheme 1[a]

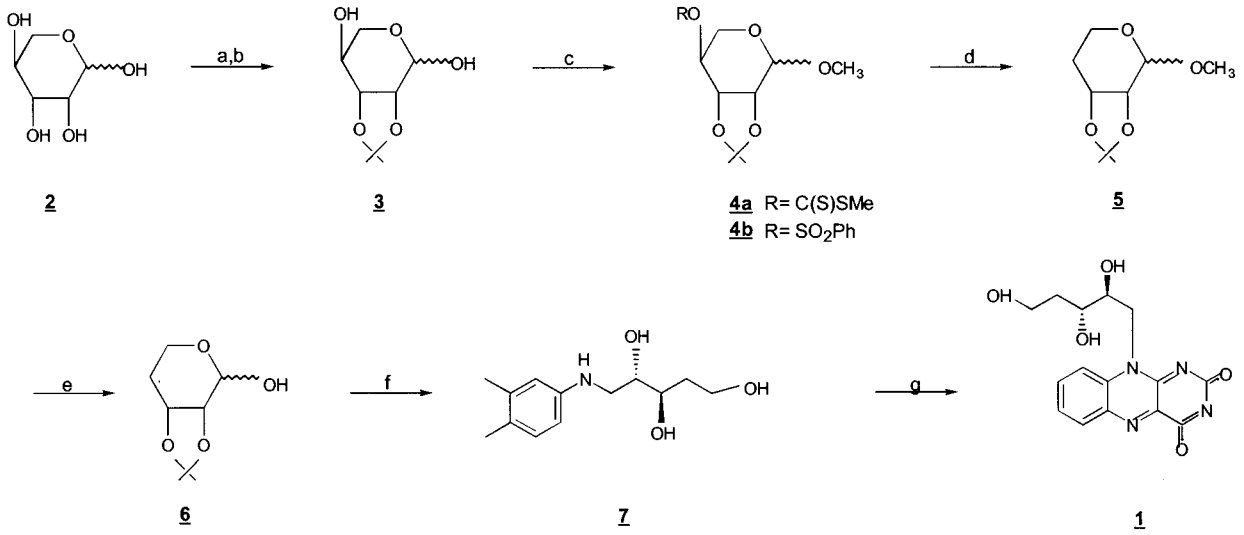

[a] Reagents and conditions: (a) HCl/MeOH; (b) 4.5 M HCl in dioxane (78% in two steps)/2,2-dimethoxyethane; (c) NaH, CS_2 then MeI (100%) for **4a**, and PhOSOCl, Py, 25 °C for **4b**; (d) Bu_3SnH, toluene (80%); (e) acOH/H_2O (1:1 v/v) at 55−60 °C, then at 115 °C (95%); (f) (I)3,4-dimethylaniline, MeOH, reflux, (II) 10% Pd/C, H_2 (52% in two steps); (g) benzene diazonium chloride, work-up then barbituric acid, *n*-BuOH/AcOH, then HPLC.

(1H, m), 4.13 (1H, dd, J = 6.0, 2.7 Hz), 3.87−3.82 (2H, m), 3.73−3.71 (1H, m), 3.47 (3H, s), 2.90 (1H, bs, −OH), 1.52 (3H, s), 1.36 (3H, s).

*Step 2. Synthesis of (3aR,7S,7aS)-4-Methoxy-2,2-dimethylperhydro[1,3]dioxolo[4,5-c]pyran-7-yl Phenyl Sulfite (**4b**).* To a mixture of the hydroxyacetonide **3** (1.425 g, 7.04 mmol) and a catalytic amount of 4-(dimethylamino)pyridine (50 mg) in pyridine was added 1-(chlorosulfinyloxy)benzene (1.5 g, 8.5 mmol) dropwise under nitrogen at 0 °C. The cold bath was removed, and the mixture was magnetically stirred at room temperature overnight. Pyridine was removed under high vacuum. Standard workup of the residue with ether followed by evaporation gave the acetonide **4b** in essentially quantitative yield, which was taken to the next step without purification. Large scale reactions were carried out using the standard Barton procedure (*23*) with similar results. ^{1}H NMR ($CDCl_3$) 7.44−7.4 (2H, m) 7.32 (1H, m), 7.12 (2H, d, J = 8.5 Hz), 5.49 (1H, m), 4.70 (1H, d, J = 3.0 Hz), 4.44 (1H, t, J = 5.5 Hz), 4.15 (1H, dd, J = 5.5, 3.0 Hz), 3.92 (1H, dd, J = 11.8, 4.5 Hz), 3.83 (1H, dd, J = 11.8, 7.4 Hz), 3.46 (3H, s), 1.58 (3H, s), 1.40 (3H, s).

*Step 3. Synthesis of (3aR,7aR)-2,2-Dimethylperhydro[1,3]dioxolo[4,5-c]pyran-4-yl Methyl Ether (**5**).* The crude thioacetonide (2.38 g, 7.04 mmol) was dissolved in anhydrous toluene (45 mL) under nitrogen. Tri-*n*-butyltin hydride (3.55 mL, 10.56 mmol) and azobisisobutyronitrile (100 mg) were added, and the mixture was stirred under reflux for 2 h. Rotary evaporation gave an oil which was chromatographed using 10−15% ethyl acetate/hexane to furnish **5** as a colorless oil. ^{1}H NMR ($CDCl_3$) 4.46 (2H, d, J = 4.7 Hz), 4.38 (1H, dd, J = 9.7, 4.77 Hz), 3.86 (1H, t, J = 4.8 Hz), 3.78 (1H, m), 3.64 (1H, m), 3.47 (3H, s), 2.0 (1H, m), 1.89 (1H, m), 1.54 (3H, s), 1.36 (3H, s).

*Step 4. Synthesis of (3S,4S)-2-Methoxytetrahydro-2H-3,4-pyrandiol (**6**).* The deoxygenated acetonide **5** dissolved in AcOH/H_2O (1:1 v/v, 0.2 M) was heated first at 55−60 °C overnight and then at 110 °C (bath temperature) for 6 h under nitrogen. After removal of the volatiles, the material was coevaporated with toluene to remove residual acetate. The viscous oil **6** was judged suitable for the next step. ^{1}H NMR (D_2O) 4.68 (1H, d, J = 3.9 Hz), 4.03 (1H, m), 3.76 (2H, m), 3.65 (1H, t, J = 3.6 Hz), 3.45 (3H, s), 1.85 (1H, m), 1.75 (1H, m).

*Step 5. Synthesis of (3R,4R)-5-(3,4-Dimethylanilino)-pentane-1,3,4-triol (**7**).* Crude **6** (181 mg, 1.35 mmol) and 3,4-dimethylaniline were dissolved in 25 mL of anhydrous methanol (distilled from magnesium methoxide) and heated under nitrogen at 70 °C for 3 h. After the solution was cooled, 60 mg of 10% Pd−C was added, and the mixture was hydrogenated at room temperature and 1 atm pressure for 16 h. After filtration through Celite, the volatiles were removed under reduced pressure. Chromatography (serial elution with 80% ethyl acetate/hexane, then with ethyl acetate and finally with 10% methanol/ethyl acetate) afforded the triol **7** in 56% yield. ^{1}H NMR ($CDCl_3$) 6.91 (1H, d, J = 8.1 Hz), 6.46 (1H, d, J = 2.1 Hz), 6.41 (1H, dd, J = 8.0, 2.1 Hz), 4.15−3.70 (10H, m), 3.25 (1H, dd, J = 12.6, 3.3 Hz), 3.08 (1H, dd, J = 12.6, 7.8 Hz), 2.16 (3H, s), 2.13 (3H, s), 1.72 (2H, m).

*Step 6. Synthesis of 4′-Deoyriboflavin (**1**).* 4′-Deoxyriboflavin was then synthesized from **7** using the condensation reaction of Tischler et al. (*24*). The orange-yellow material, thus obtained, did not require any further purification as judged by its spectral properties. However, analysis by thin-layer chromatography showed a small amount of an unknown impurity. The material was further purified by HPLC on a Vydac C_8 column (5 μ, 2.2 × 25 cm) by elution with a gradient of 0−40% acetonitrile in water over 40 min with a flow rate of 10 mL/min. The product had the absorption spectrum of authentic riboflavin, λ_{max} = 254 nm. The yield was 75 mg. ^{1}H NMR (Me_2SO-d_6) 11.34 (1H, s, -nh), 7.89 (1H, s), 4.97 (1H, −OH, d, J = 4.8 Hz), 4.90 (1H, −OH, d, J = 5.5 Hz), 4.77 (1H, bd), 4.66 (1H, dd, J = 11.0, 9.0 Hz), 4.43 (1H, −OH, t, J = 4.8 Hz), 3.89 (1H, m), 3.68 (1H, m), 3.59 (2H, m), 2.50 (3H, s), 2.40 (3H, s), 1.89 (1H, m), 1.55 (1H, m). ESI−MS (361, $M^+ + 1$).

Construction and Cultivation of a Flavokinase/FAD-synthetase Expression Strain. The flavokinase/synthetase

gene (accession number: D37967) coding for the bifunctional enzyme flavokinase/FAD-synthetase of *Corynebacterium ammoniagenes* was amplified by PCR from the chromosomal DNA of the *C. ammoniagenes* strain DSM 20305 with primers FAD(CA)-1 and FAD(CA)-2, which introduced recognition sites for the restrcition enzymes, EcoRI and BamHI, at the ends of the gene: (primer FAD-(CA)-1, 5′- TCAGAATTCCATGGATATTTGGTACGG-3′; primer FAD(CA)-2, 5′-GGCCAACGCAAAGGGATCCTC-GATACC-3′). The PCR product of 1006 base pairs was digested with EcoRI and BamHI and ligated into vector pMal-c2 (New England Biolabs), which had also been treated with EcoRI and BamHI, thus yielding the plasmid, pMalribF-(CA). The recombinant *Escherichia coli* XL-1 blue strain carrying plasmid pMalribF(CA) was grown in Luria-Bertani medium, containing ampicillin (170 mg/L) to an optical density of 0.6 at 600 nm. Isopropyl-thio-β-D-galactopyranoside (Sigma) was added to 1 mM, and incubation was continued for 3 h with shaking at 37 °C. After the cells were harvested by centrifugation (5000 rpm, 15 min, 4 °C), the cells were disrupted by sonication, yielding the crude cell extracts.

Conversion of 4′-Deoxyriboflavin to 4′-Deoxy-FAD. A 3 mL sample of an agarose/amylose resin (New England Biolabs) was incubated with 8 mL of a crude cell extract of the recombinant strain for 5 min in 50 mM Tris-HCl, pH 7.5. The cell extract was removed by centrifugation (3000 rpm, 10 min, 4 °C), and the amylose resin containing the bifunctional enzyme was washed twice with 10 mL of 50 mM Tris-HCl, 100 mM NaCl, pH 7.5. The amylose resin suspension was added to a solution containing 1.3 mM 4′-deoxyriboflavin, 13 mM ATP, 10 mM $MgCl_2$, and 50 mM Tris-HCl, pH 7.5 in a total volume of 10 mL. The solution was incubated at 37 °C for 8 h with gentle shaking. The amylose-bound protein was removed by centrifugation (3000 rpm, 10 min, 4 °C), and the 4′-deoxy-FAD was purified by preparative HPLC on a RP 19 Nucleosil column (15 × 250 mm). The column was developed with an eluent containing 12% methanol and 50 mM ammonium bicarbonate. Fractions containing 4′-deoxy-FAD were concentrated under reduced pressure, and ammonium bicarbonate was removed by lyophilization. The purified 4′-deoxy-FAD was then analyzed by HPLC on a Microsorb C_{18} column (5 μm, 4.5 × 250 mm) at a flow rate of 0.5 mL/min. The column was eluted with with 20% methanol in 10 mM potassium phosphate, pH 6.0, for 15 min followed by a gradient of 20−55% methanol in the potassium phosphate buffer run over 45 min. 4′-Deoxyriboflavin and the 4′-deoxy-FAD were eluted at 44.6 and 26.2 min, similar to authentic riboflavin and FAD (45.2 and 26.8 min). The deoxy analogues also had the same mobilities as the authentic flavins when analyzed by thin-layer chromatography on silica gel developed with 10% dibasic sodium phosphate. Analysis of authentic FAD and 4′-deoxy-FAD by electron spray ionization (±) mass spectroscopy gave positive molecular ions ($M^+ + 1$) of 786 and 770, respectively, and negative ions ($M^- - 1$) of 784 and 768, respectively, in agreement with expected results for the deoxy analogue. UV-vis spectra of the analogue showed maxima at 449, 376, and 265 nm (0.30:0.23:1.00), which are essentially identical to authentic FAD (0.30:0.24:1.00).

Preparation of Human apoETF and Reconstitution of the apoETF with 4′-deoxy-FAD. ApoETF containing AMP was prepared by treatment of holoETF with buffered 3 M KBr (*12*). The apoprotein was separated from FAD and KBr on tandem 5 mL columns of Sephadex G-25 (HiTrap; Pharmacia) by elution with 50 mM potassium phosphate, pH 7.5, containing 5% glycerol using a Pharmacia FPLC system. The apoprotein contained no detectable FAD, and the concentration of apoprotein was determined using $\epsilon_{272nm} = 3.94 \times 10^4\ M^{-1}cm^{-1}$ (*12*). The apoprotein was reconstituted with a 10% molar excess of 4′-deoxy-FAD at 4 °C for 16 h. Unbound flavin nucleotide was removed from the incubation mixture by repeated concentration of the protein from 50 mM potassium phosphate, pH 7.5, containing 5% glycerol, using a Centriprep30 (Amicon) until flavin could not be detected fluorometrically in the filtrate. The yield of reconstituted ETF was always about 50%, and analysis of the nucleotide content of the protein by HPLC (*12*) after heat denaturation in the dark showed 4′-deoxy-FAD and AMP in equimolar concentrations (*12*). The A_{270nm}:A_{436nm} of the native protein was 5.9−6.0. By comparison, the A_{270nm}:A_{443nm} ratio of the reconstituted protein was 6.4−6.5, indicating that there was little denatured protein in the preparations. Moreover, the AMP:FAD ratio of the preparations was always about 1:1. If the preparations had contained significant levels of denatured protein or unreconstituted apoprotein, then the level of AMP would be increased since the removal of FAD with KBr does not remove AMP. Presumably, denatured protein is deposited on the surface of Centriprep or Centricon filters during concentration and removal of unbound 4′-deoxy-FAD.

Steady-State Kinetic Assays. Medium-chain acyl-CoA dehydrogenase was assayed spectrophotometrically with native human ETF or 4′-deoxy-FAD reconstituted ETF as a varied substrate, 50 mM octanoyl CoA and 2,6-dichlorophenolindophenol ($\epsilon_{600nm} = 2.1 \times 10^4\ M^{-1}\ cm^{-1}$) (Sigma) as the terminal electron acceptor (*19*). The dehydrogenase was also assayed spectrophotometrically under anaerobic conditions by following the formation of ETF semiquinone at 373 nm using $\Delta\epsilon_{sq-ox} = 5.1 \times 10^3\ M^{-1}\ cm^{-1}$ (*18*) for the wild-type protein and $6.1 \times 10^3\ M^{-1}\ cm^{-1}$ for the analog-containing protein. ETF-QO was assayed spectrophotometrically as a ubiqionone reductase with ETF or 4′-deoxy-FAD containing ETF as a varied substrate; substrate concentrations of medium-chain acyl-CoA dehydrogenase (1 mM), octanoyl-CoA (50 mM), and ubiquinone-1 (70 mM) were as previously described (*21*). ETF-QO was also assayed spectrophotometrically by the disproportionation of ETF semiquinone (*25*), using the molar absorptivities of the oxidized, semiquinone, and hydroquinone oxidation states of the wild-type protein previously reported (*18*). The molar absorptivities of the oxidized and semiquinone oxidation states of ETF containing 4′-deoxy-FAD are reported in Results. It was very difficult to reduce the analog-containing ETF to the hydroquinone form, and the molar absorptivity of wild-type ETF hydroquinone was assumed in calculating the rate of disproportionation of the analog-containing protein (*25*). ETF reduction by ETF-QO (the reverse reaction) was assayed as an NADH-ETF reductase with submitochondrial particles under anaerobic conditions in the presence of 1 mg of antimycin A, 1 mM *m*-carbonylcyanide chlorophenylhydrazone, 70 mM NADH, and 4 mM ETF. ETF is reduced to the semiquinone under these assay conditions, and the reaction is totally inhibited by rotenone and antibody to ETF-

QO (*22*). Activity was determined on a Hewlett-Packard 8452a diode array spectrophotometer at 436 nm for wild-type ETF, or 443 nm for the analog-containing ETF, using $\Delta\epsilon = 9.4 \times 10^3$ (*18*) or 8.6×10^3 M^{-1} cm^{-1}, respectively. Isosbestic points for the oxidized/semiquinone states at 404 and 484 nm for the wild-type ETF were maintained throughout the assay.

Spectroscopy. UV−vis absorption spectra were routinely determined with a Shimadzu UV2401 spectrophotometer. ETF flavin fluorescence emission spectra were determined on a Shimadzu RF5302 fluorescence spectrophotometer at 25 °C. Native human ETF was excited at 436 nm, and emission was measured from 450 to 560 nm. ETF containing 4′-deoxy-FAD was excited at 443 nm, the absorption maximum, and fluorescence was measured from 480 to 560 nm. Flavin circular dichroism spectra were determined with an AVIV 60DS spectropolarimeter at 4 °C as previously described (*12*).

Determination of Association Constants. The bindings of 4′-deoxy-FAD and FAD were determined by spectrophotometric and fluorimetric titrations of the coenzymes with concentrated apoprotein (50−80 mM) at 25 °C. In the fluorometric titrations, 1 mM FAD or 4′-deoxy-FAD in 10 mM bis-Tris, pH7.0, was titrated with apoprotein; a control containing FAD or the analogue was titrated with buffer in parallel. Flavin binding was determined from flavin fluorescence quenching with excitation at the visible absorption maxima and emission at 490 nm for native ETF and 520 nm for the analog-containing ETF. In the spectrophotometric titrations, 3 mM FAD or the 4′-deoxy analogue was titrated with apoprotein and the difference in absorbance at 440 nm for the 4′-deoxy-FAD and 434 nm for FAD was determined. A control incubation containing FAD or the analogue was titrated with buffer. Binding constants were calculated as described by Heyn and Weischet (*26*).

Determination of Redox Potentials. The two-electron potentials of FAD and 4′-deoxy-FAD (50 mM) were determined by cyclic voltammetry in 50 mM potassium phosphate, pH 7.0, with a gold electrode and an Omni 90 potentiostat (Cypress Systems, Inc.), using a scan rate of 0.1 V/s at room temperature.

The redox potential for the oxidized/semiquinone couple of ETF containing 4′-deoxy-FAD was estimated by the xanthine/xanthine oxidase method of Massey (*27*), using resorufin ($E'_0 = -0.051$ V) (*28*) as the indicator dye. Reactions were conducted at 10 °C, in reaction mixtures containing 10 mM potassium phosphate, pH 7.0, 10% ethylene glycol, 200 μM xanthine, 2 μM benzyl viologen, 60 nM xanthine oxidase, 10 mM ETF, and 10 mM resorufin. The potential of the oxidized/semiquinone couple was determined graphically as described by Minneart (*29*) from the decrease in absorbance at 572 nm due to the dye and increased absorbance at 373 nm due to reduction of the flavoprotein protein to the semiquinone. The potential of the semiquinone/hydroquinone couple was calculated from the maximum percentage of semiquinone formed reported by Husain et al. (*30*) based on the equations of Clark (*28*).

Other Analytical Methods. The molar absorptivity of bound 4′-deoxy-FAD was determined after release of the coenzyme from the protein with 5% SDS (*31*). The molar absorptivity of the corresponding semiquinone was determined by reduction of the analog-containing protein with the xanthine/xanthine oxidase system (*27*).

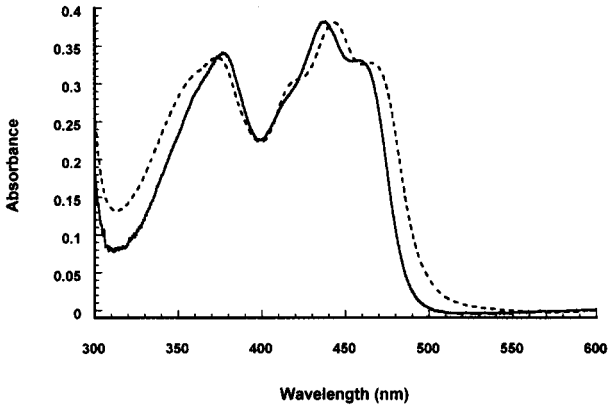

FIGURE 2: Visible absorption of human ETF containing FAD and 4′-deoxy-FAD. Human apoETF was prepared by treatment with buffered 3 M KBr and the apoprotein isolated by chromatography on Sephadex G-25. The apoETF was then reconstituted with 4′-deoxy-FAD as described in Experimental Procedures. The spectra of the wild-type human ETF, 29 μM, (− − −) and ETF reconstituted with 4′-deoxy-FAD, 27 μM, (---) were determined in 10 mM potassium phosphate buffer, pH 7.0, containing 10% glycerol.

Table 1: Spectral Properties of the Bound Flavins in the Oxidized and Anionic Semiquinone States of Human Electron Transfer Flavoprotein Containing FAD and 4′-deoxy-FAD

	FAD (mM^{-1} cm^{-1})			4′-deoxy-FAD (mM^{-1} cm^{-1})	
	oxidized	semiquinone		oxidized	semiquinone
436 nm	13.3	3.9	443 nm	14.4	5.8
373 nm	12.7	17.8	373 nm	12.5	18.7

RESULTS

Spectral Analysis of 4′-Deoxy-FAD ETF. The UV−vis spectrum of the apoETF reconstituted with 4′-deoxy-FAD was similar to native ETF with the typically resolved absorption spectrum of the bound flavin (Figure 2). However, the 436 nm maximum of the native protein was shifted to 443 nm in the analog-containing ETF, while the 373 nm maximum remained unchanged. The shifted absorption maximum is not the result of reconstitution protocol. Our previous work with human ETF and *Paracoccus* ETF showed that the absorption spectra of the bound FAD are not altered by this treatment (*12*, *15*), and the spectra of FAD and the analogue are identical in solution. The extinction coefficients of the native and reconstituted proteins in the oxidized and semiquinone states are given in Table 1. The 7 nm red-shifted maximum in the lower energy visible transition of the analog-containing ETF, with no significant change in the higher energy transition, is consistent with the predicted behavior of flavin that is not hydrogen bonded at N(1) (*32*). These data, and the retention of the resolved spectrum, suggest that interpretation of data is not complicated by other changes in flavin binding. Figure 3 shows the reduction of ETF containing 4′-deoxy-FAD by xanthine/xanthine oxidase/benzyl viologen. The protein stabilizes an anionic flavin semiquinone with a maximum at 373 nm. Spectrum 5 reflects 96% semiquinone. The reduction of the semiquinone to the dihydroflavin is extremely slow. Spectra labeled 6 and 7 in Figure 3 were recorded 100 and 205 min after spectrum 5. In no experiment was full reduction achieved with xanthine/xanthine oxidase or with $Na_2S_2O_4$ before the protein began to denature. The inset of Figure 3 indicates the changes in

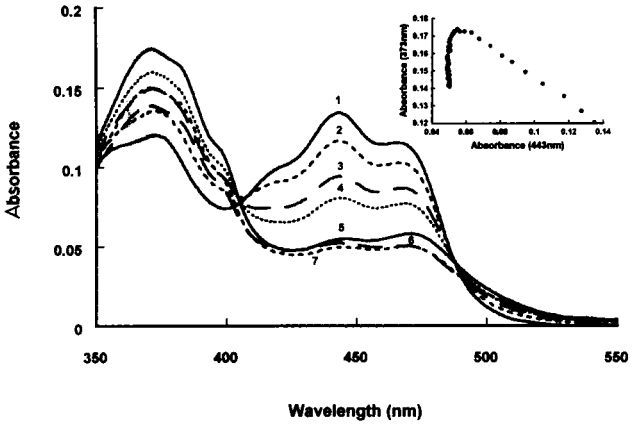

FIGURE 3: Reduction of human ETF containing 4′-deoxy-FAD. The oxidized protein [1], 10 mM, was reduced with xanthine/xanthine oxidase/benzyl viologen under anaerobic conditions at 10 °C in 10 mM potassium phosphate, containing 10% ethylene glycol as described in Experimental Procedures. Spectra were recorded at 3 min intervals; some spectra are omitted for clarity although all of the individual points at 438 and 373 nm are shown in the inset. Spectra shown were recorded at [2] 6 min, [3] 12 min, [4] 18 min, and [5] 36 min; the spectra [6] and [7] were recorded at 135 and 240 min, respectively. The inset shows absorbance at 443 and 373 nm, the maxima of the oxidized and semiquinone species, respectively, throughout the experiment.

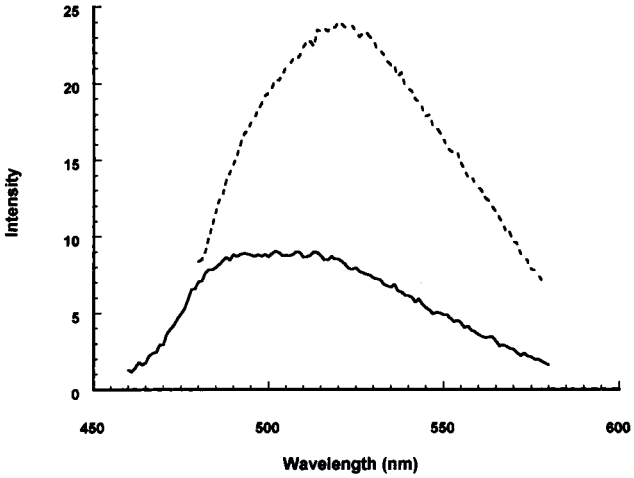

FIGURE 4: Flavin fluorescence spectra of human ETF containing FAD and 4′-deoxy-FAD. ApoETF was prepared as described in the legend of Figure 1 and reconstituted with 4′-deoxy-FAD. The recombinant human ETF (—) was excited at 436 nm and the reconstituted protein (---) was excited at 443 nm, the absorption maximum of 4′-deoxy-FAD in the reconstituted protein. Spectra of 1 μM protein were determined in 10 mM potassium phosphate, pH 7.0, containing 10% glycerol.

absorption at the maxima of the oxidized flavin (443 nm) and the flavin semiquinone (373 nm).

Analysis of the 4′-deoxy-FAD reconstituted ETF by fluorescence spectroscopy also indicated a change in the flavin environment. The intensity of the emission spectra of the reconstituted protein is approximately 2-fold greater, with λ_{max} shifted to 520 nm, similar to that of FAD in solution (Figure 4). The emission maximum of flavin in the native protein is 493 nm. The fluorescence spectra of free FAD and 4′-deoxy-FAD in solution are identical.

Finally, there was a marked difference in the flavin circular dichroism spectrum of the reconstituted protein (Figure 5). The induced circular dichroism spectrum of bound FAD can be produced by coupling of transition dipoles of the flavin

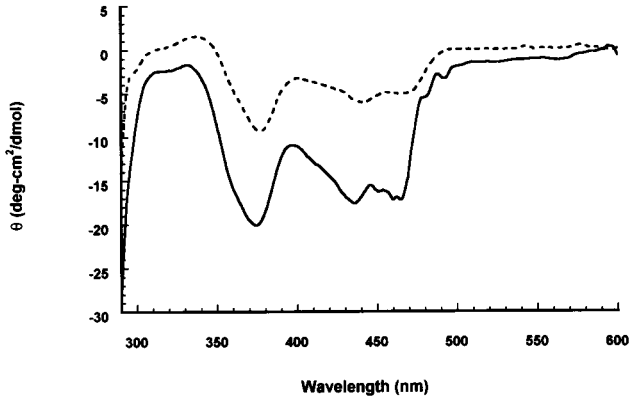

FIGURE 5: Flavin circular dichroism spectra of ETF containing FAD and 4′-deoxy-FAD. Spectra were determined in 10 mM potassium phosphate, pH 7.0, containing 10% glycerol at 10 °C. The spectra of human ETF containing FAD (—) and 4′-deoxy-FAD (---) are shown.

ring with protein-based electronic transitions, including those from the ribityl side chain, peptide bonds, aromatic amino acid side chains, and side chains of cystine and methionine (*33*−*35*). Flavin dipoles are oriented approximately from C7 to N1 for the low energy, visible transition ($\lambda_{max} \gg 450$ nm) and from C8 to N3 for the higher energy transition ($\lambda_{max} \gg 370$ nm) in the visible region (*36*, *37*). In solution, "through space" and "through bond" interactions of the isoalloxazine ring with the ribityl side chain influence the circular dichroism spectrum of free riboflavin (*37*). The chiral centers at 2′, 3′, and 4′ affect the low energy transition in a "through space" fashion. The second transition is susceptible to "through chain" interaction with the ribityl side chain. There are marked reductions in amplitude of the signals at both transitions in the analog-containing ETF. Substitution of 4′-deoxy-FAD in ETF also alters the ratio of amplitudes of the higher energy transition to the lower energy transition from 1.1 to 1.5. The altered spectrum is apparently due to a combination of "through chain" and "through space" effects due to the loss of a chiral center at C4′and the loss of the 4′-ribityl-hydroxyl-N(1) hydrogen bond.

Association Constants of FAD and 4′-Deoxy-FAD. The binding of FAD and 4′-deoxy-FAD to the ETF apoprotein was determined by titration of the flavin nucleotides with apoETF. Association constants were determined by fluorometric (Figure 6) and spectrophotometric titrations, which gave essentially identical results. The association constants for FAD and 4′-deoxy-FAD determined in the fluorometric titration were $(4.5 \pm 0.9) \times 10^6$ and $(1.9 \pm 0.6) \times 10^6$ M^{-1}, respectively. The association constants determined from spectrophotometric titrations were $(3.1 \pm 0.9) \times 10^6$ and $(1.4 \pm 0.4) \times 10^6$ M^{-1} for FAD and 4′-deoxy-FAD, respectively. These values yield a difference in binding energy of −2.1 kJ/mol favoring the binding of the natural coenzyme. This is less than the energy of an average hydrogen bond, approximately −18.8 kJ/mol. These data indicate that the intra-cofactor hydrogen bond does not play a major role in the association of the oxidized cofactor with the apoprotein. Further, the data indicate that the difference in oxidation−reduction potentials of the bound flavin between the native and analog-containing ETFs are not due to a difference in binding the oxidized coenzyme.

Redox Properties of 4′-Deoxy-FAD Reconstituted ETF. The potentials of 4′-deoxy-FAD and FAD for two-electron

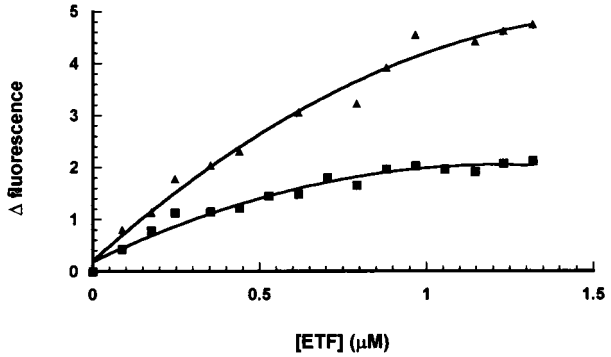

FIGURE 6: Determination of the association constants by titration of FAD and 4′-deoxy-FAD with apoETF. ApoETF was prepared as described in the legend of Figure 1. 1 μM 4′-deoxy-FAD (Δ) and 1 μM FAD (□) were titrated with apoETF as shown. Association constants were calculated from the data as described by Heyn and Weischet (*26*).

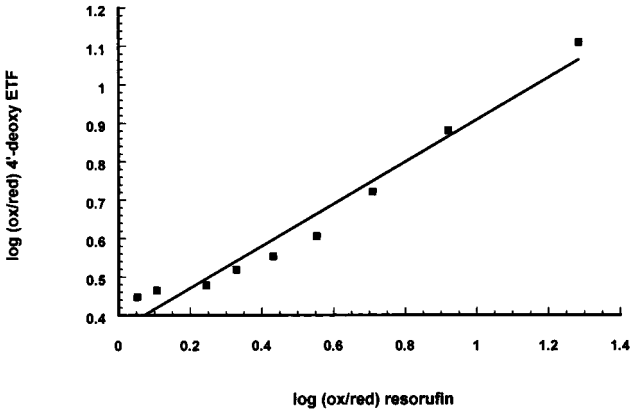

FIGURE 7: Determination of the oxidation−reduction potential of the oxidized/semiquinone couple of human ETF containing 4′-deoxy-FAD. The potential of the oxidized/semiquinone redox couple was determined by the xanthine/xanthine oxidase method of Massey (*27*) using 20 μM ETF containing 4′-deoxy-FAD, with equimolar resorufin, 200 μM xanthine, 2 μM benzyl viologen, and 30 nM xanthine oxidase in 10 mM potassium phosphate, pH 7.0, containing 10% ethylene glycol. Reactions were run at 10 °C.

transfer were determined in aqueous solution at pH 7.0 by cyclic voltammetry. The potential of the analogue was −0.203 V and the potential of FAD was −0.206 V, the latter in agreement with literature values. Therefore, differences in the redox behavior of the protein-bound FAD and 4′-deoxy-FAD can be attributed to differences in interactions of the flavin when bound to the protein resulting from the absence of the 4′-hydroxyl rather than any intrinsic difference between the potentials of the natural coenzyme and the analogue.

When the analog-containing ETF was reduced anaerobically by 50 mM octanoyl-CoA with catalytic medium-chain acyl-CoA dehydrogenase, only 27% ETF semiquinone was stabilized. This is in contrast to about 80% stabilization of the semiquinone in the native protein when reduced under the same conditions. These data suggested a change in the potentials of the analog-containing ETF.

The potential of the oxidized/semiquinone couple (Figure 7), estimated by the xanthine/xanthine oxidase method of Massey (*28*), is -0.079 ± 0.001V ($n = 3$) (Figure 6), and the estimated potential of the semiquinone/hydroquinone couple is −0.107 V, based on the stabilization of 46% semiquinone. However, the latter value is only an estimate

Table 2: Summary of Kinetic Properties of Medium-Chain Acyl-CoA Dehydrogenase and ETF-QO with FAD and 4′-deoxy-FAD as Substrates

	ETF-FAD	ETF-4′-deoxy-FAD
medium-chain acyl-CoA dehydrogenase		
V (s^{-1})[a]	14.0 ± 0.3	13.4 ± 1.0
K_m^{ETF} (μM)[a]	0.10 ± 0.02	0.3 ± 0.1
V (s^{-1})[b]	49.5 ± 6.8	11.7 ± 1.8
ETF-QO (acyl-CoA/Q_1 reductase)		
V (s^{-1})	135.1 ± 9.1	≤0.1
K_m^{ETF} (μM)	11.3 ± 1.7	
ETF-QO (ETF_{1e-} disproportionation)		
V (s^{-1})	163 ± 17	≤0.2[c]
$K_m^{ETF\ sq}$	5.8 ± 1.8	
ETF-QO (NADH-ETF reductase)[d]		
V (nmol/min/mg)	37.9 ± 5.0	≤0.2

[a] Assayed with 2,6-dichlorophenolindophenol as terminal electron acceptor. [b] Assayed with an initial ETF concentration of 4 μM by following the rate of formation of ETF semiquinone spectrophotometrically. [c] Assayed at 21 μM ETF semiquinone following the rate of ETF semiquinone disproportionation. [d] Assayed with submitochondrial particles.

because it was very difficult to fully reduce the analog-containing protein to the two-electron form with either sodium dithionite or the xanthine/xanthine oxidase system. Titration with dithionite repeatedly resulted in precipitation of the protein after only about 20% hydroquinone was formed. When the protein was reduced with the xanthine/xanthine oxidase/benzyl viologen system (*28*), the semiquinone was reduced to hydroquinone in about an 18% yield, similar to the yield during the dithionite titrations. At least 4 h was required to further reduce the semiquinone from 18% to 33% hydroquinone with the cationic reduced benzyl viologen ($E'_0 = -0.360$ V). Therefore, the potential of the semiquinone/hydroquinone couple is only an estimate and probably an overestimate.

Kinetic Properties of the 4′-Deoxy-FAD Reconstituted ETF. The steady-state kinetic constants of medium-chain acyl-CoA dehydrogenase with native ETF and ETF containing 4′-deoxy-FAD as varied substrates and 2,6-dichlorophenolindophenol as the terminal electron acceptor were almost identical (Table 2). These data indicate that flux through the analog-containing ETF was not altered when the equilibrium through the protein was displaced by recycling with the redox dye. The rate of ETF reduction to the semiquinone was also assayed spectrophotometrically. Reduction of ETF by octanoyl-CoA with catalytic medium-chain acyl-CoA dehydrogenase, at saturating ETF (4 mM) and the analog-containing ETF (4 mM) in the absence of the redox dye, showed that the steady-state rate of ETF reduction decreased 77% with the analog-containing ETF. These data may reflect the decrease in the potential of the analog-containing ETF.

In the oxidative half-reaction with ETF-QO, the turnover of ETF-QO with ETF containing 4′-deoxy-FAD is ≤0.07% of the turnover with native ETF in the acyl-CoA/ubiquinone reductase assay despite an overall favorable change in potential between the acyl-CoA/enoyl-CoA couple and the ubiquinone/dihydroubiquinone couple. Ramsay et al. demonstrated that disproportionation of ETF semiquinone to the oxidized and hydroquinone oxidation states catalyzed by ETF-QO is required in the overall reaction (*7*). Disproportionation is kinetically competent in the overall reaction. The

rate of ETF-QO catalyzed disproportionation of the analog-containing ETF was barely detectable (≤0.1% of the rate with native ETF). In the reverse reaction, ETF was reduced by NADH, submitochondrial particles as the source of ETF-QO, complex I, and ubiquinone (*22*). The exclusive product of this reaction is the ETF semiquinone and is not complicated by the participation of ETF hydroquinone. Moreover, the overall change in potential between the NAD^+/NADH couple (−0.34 V) and the potential of the analog-containing ETF oxidized/semiquinone couple (−0.079 V) indicates that the reaction is energetically favorable. However, no reduction of the 4′-deoxy-FAD containing ETF was detected. Kinetic data from assays of the reductive and oxidative half-reactions of ETF are summarized in Table 2.

DISCUSSION

The ribityl side chain of 6,7-dimethyl-8-ribityllumazine plays an essential role in the binding of ribityllumazine to riboflavin synthetase (*38*), and the ribityl side chain is very often a determinant in the binding of FMN and FAD to flavoenzymes. Only recently has the ribityl side chain of flavin coenzymes been shown to participate directly in catalysis by flavoproteins. The three-dimensional structure of medium-chain acyl-CoA dehydrogenase with bound product (*39*) demonstrated that the ribityl 2′-hydroxyl hydrogen bonds with the thioester carbonyl of the acyl-CoA substrate, suggesting that this hydrogen bond might facilitate the abstraction of the 2-*pro*-R proton by E376 to initiate the catalytic pathway. This idea was supported by studies with substrate analogues (*40*). Ghisla and co-workers directly demonstrated that the hydrogen bond activates the substrate by decreasing the pK_a of the α proton of the acyl-CoA substrate for concerted abstraction by Glu 376 and hydride transfer to the flavin (*41*). Moreover, substitution of 2′-deoxy-FAD for FAD in medium-chain acyl-CoA dehydrogenase almost completely abolished dehydrogenase activity (*42*). In lipoamide dehydrogenase, the ribityl side chain of FAD is a component of a molecular scaffold that includes tightly bound water and functional groups from the protein (*43*). Several 2′-analogues of FAD decrease the stability of the two-electron-reduced dehydrogenase and decrease the accumulation of the four-electron-reduced dehydrogenase, suggesting a significant change in redox potential of the flavin (*44*).

In human ETF (*14*) and *P. denitrificans* ETF (*9*), the 4′-hydroxyl of the ribityl side chain of FAD and N(1) of the isoalloxazine ring are within hydrogen bonding distance. Among the flavoproteins whose crystal structures are known, only pyruvate oxidase (*45*) and nitrate reductase (*46*) have FAD bound in a conformation in which the distance and geometry of 4′-ribityl-O to N(1) are consistent with hydrogen bonding. In this investigation, we studied the role of the 4′-ribityl-hydroxyl-N(1) hydrogen bond that was suggested by determination of the three-dimensional structure of human ETF by X-ray crystallography (*9, 14*) and NMR spectroscopy of ETF enriched with ^{13}C- and ^{15}N-enriched FAD (*15*). This aspect of the ETF structure was investigated directly by the incorporation of 4′-deoxy-FAD into the protein. Several points argue for the fidelity of incorporation of the analogue into the apoprotein. First, the absorption spectrum of the reconstituted protein shows the typically resolved absorption spectrum of ETF although the 436 nm absorption maximum of the native protein is shifted to 443 nm. Second, the binding constants and 4′-deoxy-FAD are essentially identical. Third, the turnover of medium-chain acyl-CoA dehydrogenase with the analog-containing ETF is very close to that determined with the native ETF if the reaction is coupled to dichlorophenolindophenol reduction. Finally, preliminary X-ray crystallographic investigations clearly show the absence of the 4′-hydroxyl group in a structure that is otherwise very similar to the native protein, including the retention of apparent hydrogen bonds of the imidazole side chain of αH286 and the backbone amide hydrogen of αR249 with the C(2)O.[2] Therefore, the changes in the properties of the flavoprotein are due to the absence of the 4′-ribityl-hydroxyl-N1 hydrogen bond.

Electrostatics, $\pi-\pi$ stacking of the flavin ring with aromatic side chains of amino acids, solvent accessibility, and conformational factors are well-known to modulate flavin redox potentials (*47*−*50*). However, hydrogen bonds, and the relative strengths of those hydrogen bonds, also control the potential of flavin in a variety of flavin host−guest model systems studied by Rotello and co-workers (*16*, *17*). The αT266M mutation in human ETF is the most frequent human mutation resulting in the metabolic disease glutaric acidemia type II (*18*). Loss of the hydrogen bond between αThr266 and N(5) of the flavin ring results in a 0.06 V decrease in the potential of the oxidized/semiquinone couple. In the present study, the intra-cofactor hydrogen bond is shown to be a major contributor in modulating the potentials of the oxidized/semiquinone and semiquinone/hydroquinone couples of the ETF flavin. The altered potentials of the 4′-deoxy-FAD containing ETF could presumably result from preferential effects on the oxidized or reduced states. The pyrimidine ring of the flavin is electron rich when reduced, and it is reasonable that the 4′-ribityl-hydroxyl-N(1) hydrogen bond may stabilize reduced species since the negative charge in the pyrimidine ring is delocalized over the N(1)−C(2)O region. Our experiments show that the energy of binding 4′-deoxy-FAD is only 2 kJ less than the binding of FAD, indicating that the decreased potential of the oxidized/semiquinone couple results from decreased stabilization of the anionic reduced forms. Further, the two-electron redox potentials of FAD and 4′-deoxy-FAD are identical in solution. Substitution of the electronegative fluorine atom in the ribityl-side chain of FAD has no effect on the two-electron potential of the flavin, indicating that the 1′-methylene group of the side chain effectively insulates the flavin from the side chain (*51*). Therefore, the changes in one-electron redox potential and kinetic properties of ETF containing 4′-deoxy-FAD are almost certainly due to the loss of the hydrogen bond at N(1).

The traditional model for stabilization of the anionic semiquinone and dihydroquinone proposed by Massey and Hemmerich (*52*) indicates stabilization from interaction with a cationic base on the enzyme. There is no such base in the vicinity of N(1) in human ETF. This is not a novel case. Medium-chain acyl-CoA dehydrogenase stabilizes a red anionic semiquinone when enoyl-CoA ligand is bound (*53*). In this protein, Thr 136 is within hydrogen bonding distance of N(1) and the carbonyl oxygen at C(2) (*39*). The hydroxyl of Thr 136 has a pK_a similar to that of the 4′-hydroxyl of

[2] Frerman, F. E. and Kim, J. J. P. Unpublished data.

Scheme 2

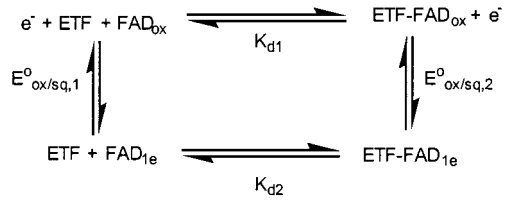

FAD. There are no cationic side chains in the region of N(1)−C(2)O in medium-chain acyl-CoA dehydrogenase. In fact, Thr 136 is maintained or conservatively substituted by a serine residue in acyl-CoA dehydrogenases. On the other hand, it is possible that the semiquinone in ETF is the neutral red semiquinone proposed by Hemmerich (*54*). However, this is not considered likely based on the absorption spectrum of ETF semiquinone (*19*), the electron paramagnetic resonance spectrum of ETF semiquinone (*55*), and the pH dependence for the disproportionation of ETF semiquinone (*25*).

From thermodynamic cycles for FAD and 4′-deoxy-FAD (Scheme 2), the contribution of the 4′-hydroxyl-N(1) hydrogen bond was estimated. The calculations assumed that the solution redox potentials of the oxidized/semiquinone couple for FAD and 4′-deoxy-FAD ($E^{o}_{ox/sq,1}$) are identical (−0.224 V (*56*)). Then, with the experimentally determined potentials of the oxidized/semiquinone couples for the proteins and the dissociation constants for FAD and the analogue, we calculated the dissociation constants for the FAD semiquinone and 4′-deoxy-FAD semiquinone, K_{d2} (Scheme 2). The ΔGs derived for these dissociation constants were −65.2 kJ/mol for FAD and −51.3 kJ/mol for 4′-deoxy-FAD with a difference in the free energy of binding between the two coenzymes of 13.9 kJ/mol. This compares with the free energy difference, 11.2 kJ/mol, calculated from the difference of 0.116 V between the oxidized/semiquinone couples.

Redox potentials within the ETF family vary widely. The potentials of pig, human, and *P. denitrificans* ETFs are near zero (*9*, *18*, *30*). In contrast, the potentials of *Methylophilus methylotrophus* ETF are +0.2 V and −0.2 V for the first and second electron transfers (*57*). The overall potential of *Megasphera elsdenii* ETF is −0.259 V (*58*). The protein stabilizes an anionic flavin semiquinone during dithionite titrations (*59*), but the semiquinone appears to be kinetically rather than thermodynamically stabilized (*58*). This is in contrast to pig, human, and methylotrophic bacterial ETFs in which the anionic semiquinones are thermodynamically stabilized (*18*, *30*, *57*). The primary sequences of the flavin binding domains (αII) of ETF subunits in these and a number of other ETFs have been determined (*9* and references therein, *60*) and are extremely conserved. Further, the predicted secondary structures surrounding the predicted and established FAD binding sites are very similar (*9*, *14*, *60*) suggesting that the FAD conformation may also be conserved. If this is the case, the difference in potentials among the ETFs implies that the 4′-ribityl-hydroxyl-N(1) hydrogen bond is more important to the stability of the anion semiquinones stabilized by these proteins than as a principal modulator of redox potential.

The loss of the 4′-ribityl-hydroxyl-N(1) hydrogen bond has no effect on the steady-state kinetic constants of medium-chain acyl-CoA dehydrogenase with the analog-containing ETF as substrate when the ETF semiquinone product is recycled with 2,6-dichlorophenol ($E_0' = +0.217$ V) as the terminal electron acceptor. However, at saturating ETF, the turnover of medium-chain acyl-CoA dehydrogenase with the analog-containing ETF is decreased 77% when ETF reduction is assayed directly. This direct assay reflects the altered potential of the oxidized/semiquinone couple of the reconstituted ETF. Thus, the analogue has no effect on the flux through the ETF when flux is made energetically favorable by coupling the reduction of ETF to dye reduction. In contrast to the reductive half-reaction with medium-chain acyl-CoA dehydrogenase, substitution of 4′-deoxy-FAD into ETF almost abolishes turnover of ETF-QO assayed in the acyl-CoA ubiquinone reductase reaction. The potential of the analog-containing ETF undoubtedly affects the turnover of ETF-QO because reduced ETF in the assay is generated with octanoyl-CoA and medium-chain acyl-CoA dehydrogenase and this reaction depends on disproportionation of ETF semiquinone catalyzed by ETF-QO (*7*). The turnover of ETF-QO in the disproportionation reaction is also barely detectable when assayed with the analog-containing ETF semiquinone. However, coupling the overall acyl-CoA/ubiquinone reductase reaction to ubiquinone ($E_0' = +0.100$ V) reduction might be expected to at least partially overcome the unfavorable disproportionation as shown above when the reduction of ETF by the dehydrogenase was coupled to dichlorphenolindophenol reduction. Electron transfer between ETF and ETF-QO was also determined in the direction of ETF reduction by ETF-QO. The reaction was assayed by following the reduction of ETF by NADH with ETF-QO in submitochondrial particles under anaerobic conditions in the presence of antimycin A to inhibit complex III. Under these conditions, ETF is reduced only to the semiquinone, the reaction is dependent on ubiquinone in the particles, and the reaction is completely inhibited by rotenone as well as antibody against ETF-QO (*22*). The low potential of the NADH/NAD^+ couple (−0.340 V) should overcome the lower potential of the analog-containing ETF oxidized/semiquinone couple (−0.079 V) so that reduction of this ETF is favorable. However, reduction to the semiquinone, when the ETF contained 4′-deoxy-FAD, was undetectable when assayed in the reverse direction.

Gorelick and Thorpe proposed that electron transfer from medium-chain acyl-CoA dehydrogenase to ETF occurs in the region of C(8) of the ETF flavin because substitution of progressively bulkier groups at C(8) results in the progressively slower rate of electron transfer from the dehydrogenase to ETF (*61*). On the basis of a model of the dehydrogease-ETF complex, which used the crystal structures of both proteins, Roberts et al. (*62*) proposed that Arg249 in the α subunit participates in the electron-transfer pathway. This model does not contradict the proposal of Gorelick and Thorpe (*61*), because the guanidinium group of αR249 makes van der Waals contact with C(9) of the flavin (*14*). The almost complete loss of oxidation−reduction activity of 4′-deoxy-ETF with ETF-QO suggests the possibility that the 4′-ribityl-hydroxyl-N(1) hydrogen bond functions in an electron tunneling pathway between the electron-rich pyridine ring of reduced ETF and the flavin of ETF-QO (*63*, *64*). Recent data indicates that electronic coupling through hydrogen bonds is greater than that provided by carbon−

carbon σ bonds (*65*−*67*). The proposal of Gorelick and Thorpe (*61*) and the results presented herein would suggest that electrons may enter and exit the ETF flavin via different pathways during the reductive and oxidative half-reactions. Different electron entry and exit pathways have also been proposed for glutathione reductase (*68*). In glutathione reductase and related proteins with redox active disulfides, electrons apparently enter from the *re* face of the flavin from reduced pyridine nucleotide at N(5) and leave on the *si* face of the flavin at C(4a).

The experiments reported in this paper support crystallographic studies (*9*, *14*) that suggested the existence of a hydrogen bond between the 4′-ribityl-hydroxyl and N(1) of the isoalloxazine ring of FAD in human and *P. denitrificans* ETFs. This hydrogen bond stabilizes the anionic semiquinone and hydroquinone forms of human ETF and thereby modulates the potentials of the two flavin oxidation−reduction couples. This hydrogen bond may also function in an electron tunneling pathway between the ETF and ETF-QO flavins. The functional significance of the 2′- and 3′-ribityl hydroxyl groups in FAD from human and *P. denitrificans* ETFs is currently under investigation.

ACKNOWLEDGMENT

We thank Dr. Jung Ja Kim for her assistance in the preparation of Figure 1. We also thank Dr. Donald Zapien and Mrs. Tiffany Hays for their assistance with the cyclic voltammetry experiments and Ms. Michelle Muller for technical assistance.

REFERENCES

1. Hauge, J. G. (1956) *J. Am. Chem. Soc. 78*, 5266−5272.
2. Izai, K., Uchida, Y., Orii, T., Yamamoto, S., and Hashimoto, T. (1992) *J. Biol. Chem. 267*, 1027−1033.
3. Ikeda, Y., and Tanaka, K. (1983) *J. Biol. Chem. 258*, 1077−1085.
4. Lenich, A. C., and Goodman, S. I. (1986) *J. Biol. Chem. 261*, 4090−4096.
5. Frisell, W. R., and McKenzie, C. G. (1964) *J. Biol. Chem. 237*, 94−98.
6. Gorelick, R. J., Schopfer, L. M., Ballou, D. P., Massey, V., and Thorpe, C. (1985) *Biochemistry 24*, 6830−6839.
7. Ramsay, R. R., Steenkamp, D. J., and Husain, M. (1987) *Biochem. J. 241*, 883−892.
8. Tsai, M. H., and Saier, M. H. (1995) *Res. Microbiol. 146*, 397−404.
9. Roberts, D. L., Salazar, D., Fulmer, J. P., Frerman, F. E., and Kim, J. J. P. (1998) *Biochemistry 38*, 1977−1989.
10. DuPlessis E. R., Rohlfs, R. J., Hille, R., and Thorpe, C. (1994) *Biochem. Mol. Biol. Int. 32*, 195−199.
11. Sato, K., Nishina, Y., and Shiga, K. (1996) *J. Biochem. (Tokyo) 120*, 276−285.
12. Griffin, K. J., Dwyer, T. M., Manning, M. C., Meyer, J. D., Carpenter, J. F., and Frerman, F. E. (1997) *Biochemistry 36*, 4194−4202.
13. Swenson, R. P., and Chen, D. (1996) in Flavins and Flavoproteins (Stevenson, K. J., Massey, V., and Williams, C. H., Jr., Eds.) pp 516−518, University of Calgary Press, Calgary.
14. Roberts, D. L., Frerman, F. E., and Kim, J. J. P. (1996) *Proc. Natl. Acad. Sci. U.S.A. 90*, 1670−1676.
15. Griffin, K. J., DeGala, G. D., Eisenreich, W., Muller, F., Bacher, A., and Frerman, F. E. (1998) *Eur. J. Biochem. 255*, 125−132.
16. Breinlinger, E., Niemz, A., and Rotello, V. M. (1995) *J. Am. Chem. Soc. 117*, 5379−5380.
17. Niemz, A., Imbriglio, J., and Rotello, V. M. (1997) *J. Am. Chem. Soc. 119*, 887−892.
18. Salazar, D., Zhang, L., deGala, G. D., and Frerman, F. E. (1997) *J. Biol. Chem. 272*, 26425−26433.
19. Herrick, K. R., Salazar, D. Goodman, S. I., Finocchiaro, G., Bedzyk, L. A., and Frerman, F. E. (1994) *J. Biol. Chem. 269*, 32239−32245.
20. Beckmann, J. D., and Frerman, F. E. (1983) *J. Biol. Chem. 258*, 7563−7569.
21. Watmough, N. J., Loehr, J. P., Drake, S. K., and Frerman, F. E. (1991) *Biochemistry 30*, 1317−1323.
22. Frerman, F. E. (1987) *Biochim. Biophys. Acta 893*, 161−169.
23. Barton, D. H. R., and McCombie, S. W. (1975) *J. Chem. Soc., Perkin Trans. 1*, 1574−1585.
24. Tischler, M., Pfister, K., Babson, R. D., Ladenberg, K., and Flemming, A. J. (1947) *J. Am. Chem. Soc. 69*, 1487−1492.
25. Beckmann, J., and Frerman, F. E. (1985) *Biochemistry 24*, 3912−3921.
26. Heyn, M. P., and Weischet, W. O. (1975) *Biochemistry 14*, 2962−2968.
27. Massey, V. (1991) in *Flavins and Flavoproteins 1990* (Curti, B., Ronchi, S., and Zanetti, G., Eds.) pp 59−66, Walter deGruyter and Co., New York.
28. Clark, W. M. (1960) in *Oxidation Reduction Potentials of Organic Systems*, p 184−203, The Williams and Wilkins Co., Baltimore, MD.
29. Minneart, K. (1965) *Biochim. Biophys. Acta 110*, 42−56.
30. Husain, M., Stankovich, M. T., and Fox, B. G. (1984) *Biochem. J. 219*, 1043−1047.
31. McKean, M. C., Beckmann, J. D., and Frerman, F. E. (1983) *J. Biol. Chem. 258*, 1866−1870.
32. Nishimoto, K., Watanabe, Y., and Yagi, K. (1978) *Biochim. Biophys. Acta 526*, 34−41.
33. Hsu, M. C., and Woody, R. W. (1971) *J. Am. Chem. Soc. 93*, 3515−3525.
34. Blauer, G., Sreerama, N., and Woody, R. W. (1993) *Biochemistry 32*, 6674−6679.
35. Edmondson, D. E., and Tollin, G. (1971) *Biochemistry 10*, 113−124.
36. Sun, M., Moore, T. A., and Song, P. S. (1972) *J. Am. Chem. Soc. 94*, 1730−1740.
37. Scola-Nagelschneider, G., and Hemmerich, P. (1972) *Z. Naturforsch. Chem. Sci. 27*, 1011−1015.
38. Plaut, G. W. E., and Beach, R. L. (1976) in *Flavins and Flavoproteins* (Singer, T. P., Ed.) pp 737−744, Elsevier Scientific Publishing, Amsterdam.
39. Kim, J. J. P., Wang, M., and Paschke, R. (1993) *Proc. Nat. Acad. Sci. U.S.A. 90*, 7523−7527.
40. Trievel, R. C., Wang, R., Anderson, V. E., and Thorpe, C. (1995) *Biochemistry 34*, 8597−8605.
41. Vock, P., Engst, S., Eder, M., and Ghisla, S. (1998) *Biochemistry 37*, 1848−1860.
42. Engst, S., Vock, P., Wang, M., Kim, J. J. P., and Ghisla, S. (1999) *Biochemistry 38*, 257−267.
43. Mattevi, A., Schierbeek, A. J., and Hol, W. G. J. (1991) *J. Mol. Biol. 220*, 975−994.
44. Murthy, Y. V. S. N., and Massey, V. (1995) *J. Biol. Chem. 270*, 28586−28594.
45. Muller, Y. A., and Schulz, G. E. (1993) *Science 259*, 965−967.
46. Lu, G., Campbell, W. H., Schneider, G., and Lindqvist, Y. (1994) *Structure 2*, 809−821.
47. Zhou, Z., and Swenson, R. P. (1995) *Biochemistry 34*, 3183−3192.
48. Zhou, Z., and Swenson, R. P. (1996) *Biochemistry 35*, 15980−15988.
49. Swenson, R. P., and Krey, G. D. (1994) *Biochemistry 33*, 8505−8514.
50. Ludwig, M. L., Pattridge, K. A., Metzger, A. L., and Dixon, M. M., Eren, M., Feng, Y., and Swenson, R. P. (1996) in *Flavins and Flavoproteins*, 1996 (Stevenson, K. J., Massey, V. and Williams, C. H., Eds) pp 409−418, University of Calgary Press, Calgary.
51. Miller, S. M. (1995) *Biochemistry 34*, 13066−13073.

52. Massey, V and Hemmerich, P. (1980) *Biochem. Soc. Trans. 8*, 246−257.
53. Mizzer, J. P., and Thorpe, C. (1981) *Biochemistry 20*, 4965−4970.
54. Muller, F., Hemmerich, P., Ehrenberg, A., Palmer, G., and Massey, V. (1970) *Eur. J. Biochem. 14*, 185−196.
55. McKean, M. C., Sealy, R. C., and Frerman, F. E. (1982) in *Flavins and Flavoproteins* (Massey, V. and Williams, C. H., Eds) pp 614−617, Elsevier, New York.
56. Lowe, H. J., and Clark, W. M. (1956) *J. Biol. Chem. 221*, 983−992.
57. Byron, C. M., Stankovich, M. T., Husain, M., and Davidson, V. L. (1989) *Biochemistry 28*, 8582−8587.
58. Pace, C. P., and Stankovich, M. T. (1987) *Biochim. Biophys. Acta 911*, 267−276.
59. Whitfield, C. D., and Mayhew, S. G. (1974) *J. Biol. Chem. 249*, 2801−2810.
60. O'Neil, H., Mayhew, S. G., and Butler, G. (1998) *J. Biol. Chem. 273*, 21015−21024.
61. Gorelick, R. J., and Thorpe, C. (1986) *Biochemistry 25*, 7092−7098.
62. Roberts, D. L., Frerman, F. E., and Kim, J. J. P. (1996) in *Flavins and Flavoproteins, 1996* (Stevenson, K. J., Massey, V. and Williams, C. H., Eds.) pp 523−526, University of Calgary Press, Calgary.
63. Paulsen, K. E., Orville, A. M., Frerman, F. E., Lipscomb, J. D., and Stankovich, M. T. (1992) *Biochemistry 31*, 11755−11761.
64. Beard, S. E., Goodman, S. I., Bemelen, K., and Frerman, F. E. (1995) *Hum. Mol. Gen. 4*, 157−161.
65. deRege, P. J., Williams, S. A., and Therien, M. J. (1995) *Science 269*, 1409−1413.
66. Bertan, D. N., and Onuchic, J. N. (1996) in *Protein Electron Transfer* (Bendall, D. S., Ed.) Chapter 2, pp 23−42, Bios Scientific Publishers Ltd., Oxford, U.K.
67. Mikkelsen, K. V., Skov, L. K., Nar, H., and Farver, O. (1993)-*Proc. Natl. Acad. Sci. U.S.A. 90*, 5443−5445.
68. Pai, E., and Schulz, G. E. (1983) *J. Biol. Chem. 258*, 1752−1757.

BI9903906